Proceedings of ASME TURBO EXPO 2002:
Land, Sea and Air
June 3 – 6, 2002 Amsterdam, The Netherlands

GT-2002-30311

3D UNSTERADY FORCES OF THE TRANSONIC FLOW THROUGH A TURBINE STAGE WITH VIBRATING BLADES

Romuald RZĄDKOWSKI
Institute of Fluid-Flow Machinery,
Polish Academy of Sciences,
Fiszera 14, PL 80-952 Gdańsk, Poland,
Polish Naval Academy

Vitaly GNESIN
Department of Aerohydromechanics,
Institute for Problems in Machinery
Ukrainian National Academy of Sciences,
2/10 Pozharsky st., Kharkov 310046, Ukraine

ABSTRACT

Numerical calculations of the 3D transonic flow of an ideal gas through turbomachinery blade rows moving relatively one to another with taking into account the blades oscillations is presented. The approach is based on the solution of the coupled aerodynamic-structure problem for the 3D flow through the turbine stage in which fluid and dynamic equations are integrated simultaneously in time, thus providing the correct formulation of a coupled problem, as the blades oscillations and loads, acting on the blades, are a part of solution. An ideal gas flow through the mutually moving stator and rotor blades with periodicity on the whole annulus is described by the unsteady Euler conservation equations, which are integrated using the explicit monotonous finite-volume difference scheme of Godunov-Kolgan and moving hybrid H-H grid. The structure analysis uses the modal approach and 3D finite element model of a blade. The blade motion is assumed to be constituted as a linear combination of the first natural modes of blade oscillations with the modal coefficients depending on time. The algorithm proposed allows to calculate turbine stages with an arbitrary pitch ratio of stator and rotor blades, taking into account the blade oscillations by action of unsteady loads caused both outer flow nonuniformity and blades motion. There has been performed the calculation for the stage of the turbine with rotor blades of 0.765 m. The numerical results for unsteady aerodynamic forces due to stator-rotor interaction are compared with results obtained with taking into account the blades oscillations.

NOMENCLATURE

IBPA	interblade phase angle [deg.],
H	source vector,
L	blade length [m],
p	pressure, [MPa],
t	temperature, [^{o}C],
δ	interblade phase angle [deg.],
χ	ratio of the fluid specific heats,
Ω	finite volume.

INTRODUCTION

The cascade flutter is characterised by aerodynamic interaction among oscillating blades in the blade row. Its importance can be understood from the fact that the unsteady aerodynamic force on blades is heavily dependent on the interblade phase angle. From this standpoint neighbouring blade rows, e. g., a neighbouring rotor or stator will have a considerable influence on the unsteady aerodynamic force because blade rows are closely placed in actual turbomachines.

A literature survey on flutter prediction methods is beyond the scope of this paper and the interested reader should consult Marshal and Imregun 1996. However, a brief overview will be given here for the sake of completeness.

Most flutter computations consider a typical sector vibrating in some given assembly mode (or interblade phase angle) for which flutter is expected to occur**.** In other words, the flutter mode must be known before the analysis, though it is also possible to consider the individual stability of each mode in turn. In such, usually linear analysis, the interblade phase angle must be prescribed at the periodic boundaries.

In recent times the new approaches based on the simultaneous integration in time of the equations of motion for the structure and the fluid are developed (Bakhle *et al*. 1992, He 1984; Moyround *et al*. 1996, Rządkowski 1998, Rządkowski and Gnesin 2000, 2001, He and Ning 1998, Bendiksen 1998, Gnesin *et al*.2000, 2001, Carstens and Belz 2000). These approaches are very attractive due to the correct formulation of a coupled problem, as the interblade phase angle at which a stability (instability) would occur is a part of solution. Generally the papers presented above take into consideration

only the rotor blades. The stator blades are modelled by the interblade phase angle of the rotor blades as the initial condition.

Hall and Silkowski 1997 can be cited as one of a few papers investigating into the effect of neighbouring blade rows. They presented an analysis based on two-dimensional multiple blade rows, in which blades of one blade row are oscillating, and showed a remarkable difference of the aerodynamic damping from that of an isolated blade row.

Namba and Ishikawa 1983 gives an analytical study on contra-rotating annular cascades with oscillating blades. In that paper the case of blade oscillation of one of the pair cascades but also the case of the blade oscillation of both cascades is considered. The analytical method is an extension of one of the authors" unsteady linearized lifting surface theory for a rotating annular cascade to the model of a pair of contra-rotating cascades. Recently the validity of the original code has bee confirmed from comparison of the Namba's data with those computed by Schulten's code 1982, both of which are submitted to the Third Computational Aeroacoustics Workshop on Benchmark Problems (November, 1999, Ohio Aerospace Institute) as analytical solutions of Category 4 Fan Stator with Harmonic Excitation by Rotor Wake.

In the present study for the first time the algorithm proposed involves the coupled solution of an aerodynamic problem for turbine stage and the dynamic problem for vibrating blades. The stage of the turbine with rotor blades of 0.765 m (blade length) were used.

AERODYNAMIC MODEL

The 3D transonic flow of inviscid non-heat conductive gas through an axial turbine stage is considered in the physical domain, including the nozzle cascade (NC) and the rotor wheel (RW), rotating with constant angular velocity. In general case both NC and RW have an unequal number of blades of the arbitrary configuration. Taking into account the flow unperiodicity from blade to blade (in the pitchwise direction) it is convenient to choose the calculated domain including all blades of the NC and RW assembly, the entry region, the axial clearance and the exit region (see Fig.1a).

The spatial transonic flow including in the general case strong discontinuities in the form of shock waves and wakes behind the exit edges of blades is written in the relative Cartesian coordinate system rotating with constant angular velocity ω according to the full non-stationary Euler equations, presented in the form of integral conservation laws of mass, impulse and energy (Godunov *et al.* 1976).

The calculated domain, including all blades on the whole annulus as well as inlet and outlet domains, consists of two subdomains (NC and RW) having the common part. Let the stator and rotor involve z_s and z_r blades respectively. So the difference grid is divided into $z_s + z_r$ difference segments, each of them includes a blade and has an expansion in circumferential direction, which is equal to the pitch of stator or rotor respectively (see Fig.1a). The subdomian *abcd* (see Fig. 1c) includes the stator blades, the subdomain *efgh* includes the rotor blades. In subdomain *efgh* the internal boundary conditions between stator and rotor blades exchange.

Each of passages are dicretized using H-type grid for stator domain and hybrid H-H grid for rotor domain (Gnesin and Rzadkowski 2000). Here outer H-grid remains stationary during the calculation, while the inner H-grid is rebuilt in each iteration by a given algorithm, so that the external points of the inner grid remain unmoved, but the internal points (on the blade surface) move according to the blade motion (see Fig 1 b).

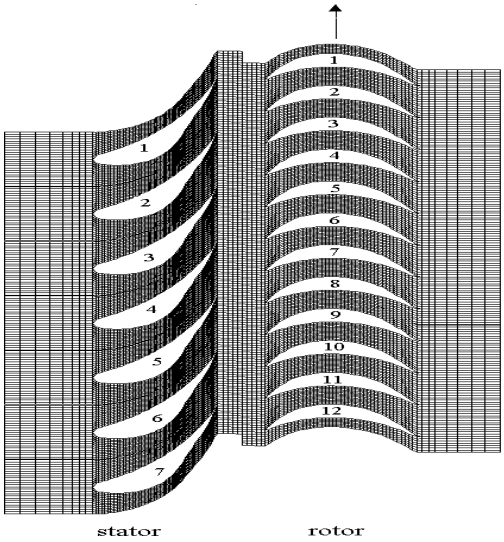

Figure 1a. The tangential section of the turbine stage

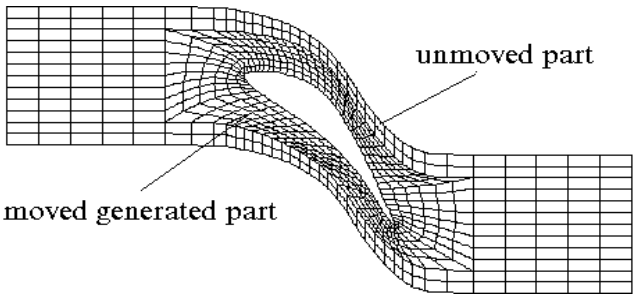

Figure 1b. The unsteady grid generation

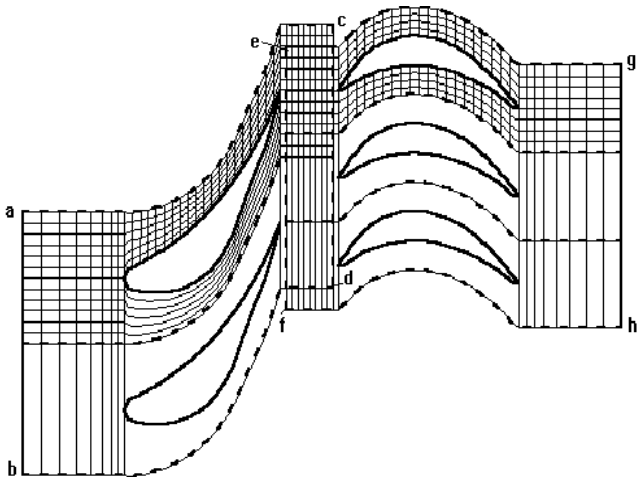

Figure 1c. The difference grid

The discretized form of governed equations was obtained on an arbitrary moving grid by Godunov idea, but in the more universal form extended for three space coordinates (Gnesin *et al*. 2000, Godunov *et al.* 1976):

$$\frac{1}{\Delta t}\Big[f^{i+\frac{1}{2},j+\frac{1}{2},k+\frac{1}{2}} \cdot \Omega^{i+\frac{1}{2},j+\frac{1}{2},k+\frac{1}{2}} - f_{i+\frac{1}{2},j+\frac{1}{2},k+\frac{1}{2}} \cdot \Omega_{i+\frac{1}{2},j+\frac{1}{2},k+\frac{1}{2}} \Big] + \\ + \Big[-(f\sigma w_n)_{i+1} + (f\sigma w_n)_i - (f\sigma w_n)_{j+1} + (f\sigma w_n)_j - (f\sigma w_n)_{k+1} + \\ + (f\sigma w_n)_k \Big] + \Big[(F_1\sigma)_{i+1} - (F_1\sigma)_i + (F_2\sigma)_{j+1} - (F_2\sigma)_j + (F_3\sigma)_{k+1} - \\ - (F_3\sigma)_k \Big] + H_{i+\frac{1}{2},j+\frac{1}{2},k+\frac{1}{2}} \cdot \Omega_{i+\frac{1}{2},j+\frac{1}{2},k+\frac{1}{2}} = 0 \quad (1)$$

The gasodynamic parameters on the lateral sides (expressions in square brackets with integer indexes) are defined using the Riemann problem of an arbitrary discontinuity on the moving interfaces between two adjacent cells and by using of the iteration process.

It is assumed that the unsteady flow fluctuations are due to both the rotor wheel rotation and to prescribed blade motions, and the flows far upstream and far downstream from the blade row are at most small perturbations of uniform free streams. So the boundary conditions formulation is based on one – dimensional theory of characteristics, where the number of physical boundary conditions depends on the number of characteristics entering the computational domain.

In the general case, when axial velocity is subsonic, at the inlet boundary initial values for total pressure, total temperature and flow angles are used, while at the outlet boundary only the static pressure has to be imposed. Nonreflecting boundary conditions must be used, i.e., incoming waves (three at inlet, one at the outlet) have to be suppressed, which is accomplished by setting their time derivative to zero.

On the blade's surface, because the grid moves with the blade, the normal relative velocity is set to zero

$$(\vec{v} - \vec{w}) \cdot \vec{n} = 0 .$$

In the general case, computations are made using a number of blade passages equal to the number of blades in the cascade. Periodic conditions are applied at the upper and lower boundaries of the calculated domain at each time moment.

STRUCTURAL MODEL

The blade vibration formulation is based on a modal approach of the coupled problem (Bathe and Wilson 1976, Rzadkowski 1998). The dynamic model of the oscillating blade in linearized formulation is governed by matrix equation:

$$[M]\{\ddot{u}(t)\} + [C]\{\dot{u}(t)\} + [K]\{u(t)\} = [F], \quad (2)$$

where [*M*] , [*C*], [*K*] are the mass, mechanical damping and stiffness matrices of the blade respectively; *{u(t)}* is the blade displacement; [*F*] is the unsteady aerodynamic forces vector, which is a function of blade displacement.

The first step of the modal approach consists of solving the problem of the natural mode shapes and eigenvalues without damping and in a vacuum. Then the displacement of each blade can be written as a linear combination of the first *N* modes shapes with the modal coefficients depending on time:

$$\{ u(t) \} = [U] \{ q(t) \} = \sum_{i=1}^{N} \{U_i\} q_i(t) \quad (3)$$

where U_i is the displacement vector corresponding to i - th mode shape; $q_i(t)$ is the modal coefficient of i - th mode. Taking into account the equation (3) and the orthogonality property of the mode shapes the equation (2) can be written in form of:

$$[I]\{ \ddot{q}(t) \} + [H]\{\dot{q}(t)\} + [\Omega]\{ q(t) \} = \{ \lambda(t) \}, \quad (4)$$

where [*I*]=diag (1, 1, ... 1), [*H*] =diag (2 h_1, 2 h_2 , ... 2 h_n), [Ω] =diag (ω_1^2, ω_2^2 , ... , ω_n^2) are diagonal matrices; ω_i is i-th natural blade frequency; { *λ(t)* }is the modal forces vector corresponding to the mode shapes, $h_i = \omega_i \xi_i$, where ξ_i is the i-th modal damping coefficient (see Bathe and Wilson 1976). Thus the dynamic problem (2) reduces to the set of independent differential equations relatively to modal coefficients of natural modes:

$$\ddot{q}_i(t) + 2h_i \dot{q}_i(t) + \omega_i^2 q_i(t) = \lambda_i(t), \quad (5)$$

The equations of motion (5) can be solved using any standard integration method.

The modal forces λ_i are calculated at each iteration with the use of the instantaneous pressure field in the following way:

$$\lambda_i = \frac{\iint_{\sigma} p \, \overline{U}_i \cdot \overline{n}^{\circ} \, d\sigma}{\iiint_{v} \rho \, \overline{U}_i^2 \, dv} . \quad (6)$$

where p is the pressure along the blade surface.

NUMERICAL RESULTS

The numerical calculations presented below were carried out for the stage of the turbine with rotor blades of L=0.765 m. The number of stator blades is equal to 56, the number of rotor blades is equal to 96. The stator to rotor blade number ratio of 56:96 (7:12). All geometrical parameters of the blade are presented in Rzadkowski 1998.

The numerical and experimental verification of the numerical code is presented in Rzadkowski and Gnesin 2000.

The numerical calculations have been made using the computational H-grid of 10*24*58 grid points for each stator passage and 10*14*58 grid points for each rotor passage. The accuracy of the numerical calculations for this grid is discussed in Gnesin, Rzadkowski and Kolodyazhnaya 2000.

One of the important aspects of stator-rotor interaction is the effect of the blade response with taking into account the excitation caused by the flow ununiformity and excitation due to blades oscillations. The low frequency response in Fig. 2 are due to blades oscillations.

In accordance with the stator/rotor ratio of blades (z_s : z_r = 7:12) we observe that the load phase lag for i-th blade comparatively to the first one is of 2π (i-1) z_s :z_r or 7/6π (i-1).

The unsteady modal forces acting on the 1st and 5th blades (see Fig.1), corresponding to the first mode and to the second mode respectively were shown in Fig 2 a,b,c,d .

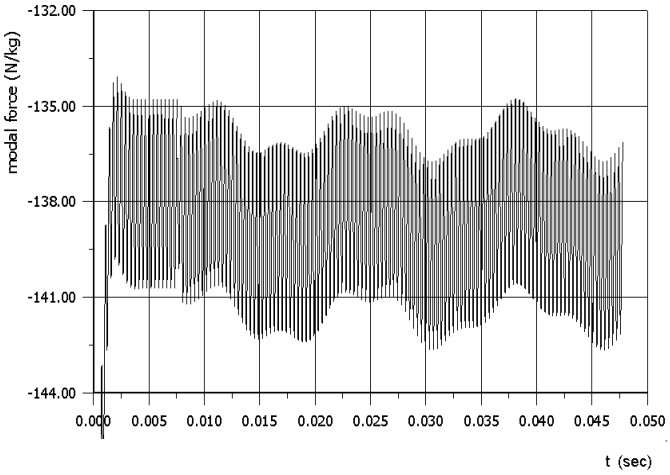

Figure 2a. The unsteady modal forces of the 1st blade corresponding to 1st mode shape, during one rotor rotation

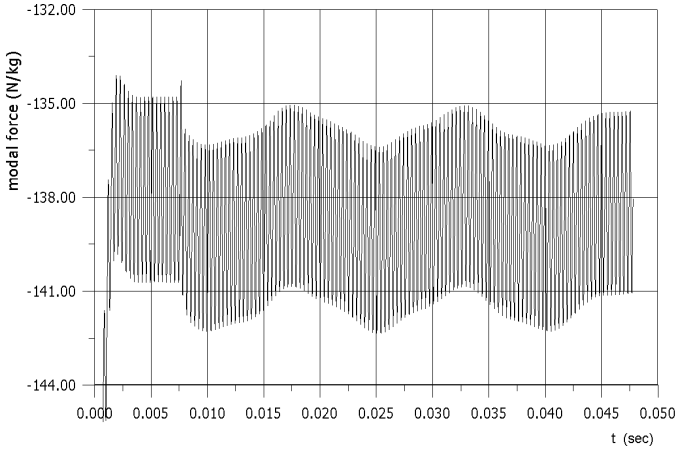

Figure 2b. The unsteady modal force of 5th blade corresponding to 1st mode shape during one rotor rotation

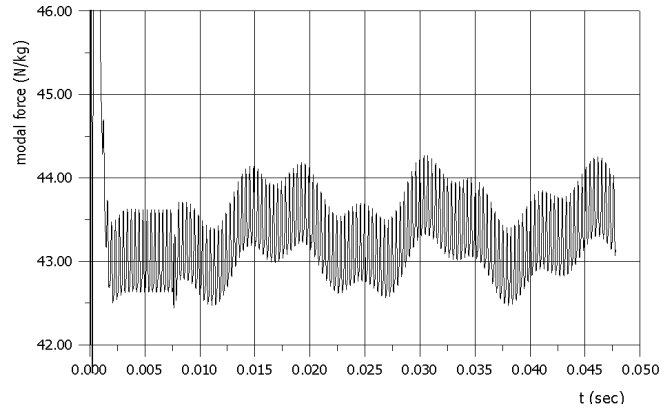

Figure 2c. The unsteady modal forces of 1st blade corresponding to 2nd mode shape during one rotor rotation

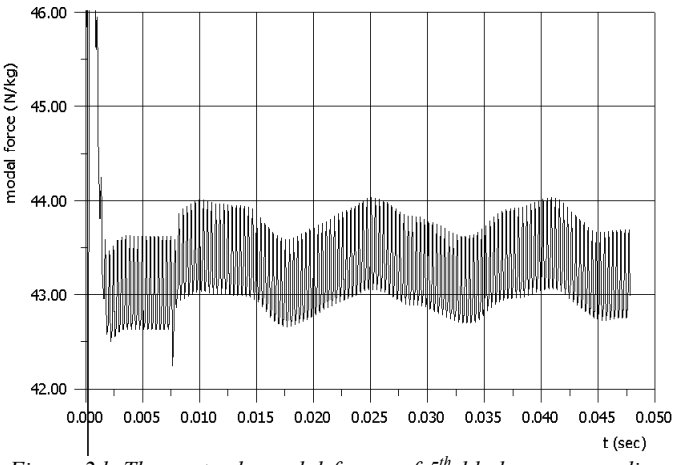

Figure 2d. The unsteady modal forces of 5th blade corresponding to 2nd mode shape during one rotor rotation

The calculation includes two regimes. In the first regime the calculation of the unsteady flow through the turbine stage with taking into account the rotor rotation, but without blade vibration, were carried out. Next the blades vibration began.

Figures 2a,b,c,d present the change of the modal forces during the time period $T=1/(50 \bullet 8)= 0.0025$ s. (where $\omega = 2\ \pi\ 50\ s^{-1}$, 56 stator blades , 7 stator blades in one section (see Fig. 1), 56 / 7=8) and corresponding to the rotor moving past seven stator airfoil pitch. This distance corresponds to 1/8 of one full rotor revolution. The zone of periodicity consists 7 rotor cycles, from 0.0050 s. to 0.0075 s. (one cycle corresponds to rotor moving past one stator airfoil pitch).

After some time moment, named as the start regime (in calculation it corresponds to time moment of 0.0075 s.) all blades start to vibrate caused by the instantaneous forces acting on them. The numerical results presented in Figures 2 correspond to the one rotation of the rotor equal in this case to 1/50 s. (t = 0.0075s, ... , 0.0275 s.).

The blade vibration are defined with taking into account the first ten natural modes shapes and the rotation of the blade. The values of natural frequencies and the mechanical damping coefficients $h_i = 2\omega_i\xi_i$, are given it Table 1. The modal damping coefficients were assumed (Rzadkowski 1998): $\xi_1 =0.00075$, $\xi_2 =0.00094$, $\xi_3 =0.0011$, $\xi_3 = \xi_4 = \xi_{10}$.

Table 1. Natural frequencies and mechanical damping coefficients of the rotating rotor blade L=0.765 m

Mode number	1	2	3	4	5
ν_i, Hz	99	160	268	297	398
h_i, Hz	0.149	0.304	0.62	0.8	1.23

Mode number	6	7	8	9	10
ν_i, Hz	598	680	862	1040	1124
h_i, Hz	2.1	2.65	3.7	4.89	5.73

The unsteady modal force includes high frequency harmonics ($\nu_k = k \bullet z_s \bullet 50$) corresponding to the rotor moving past one stator blade pitch and spectrum of low frequencies (see Fig. 1a).

The unsteady force is the unperiodic function in time. The forces acting on the various blades differ one from another (see Figs. 2 a,b, c, d). We are using here the term the unsteady modal force which is equal along the blade length and corresponds to the particular mode shape. This is disadvantage of the modal superposition calculations, where modal force averaged along the length of the blades is calculated (see equation (6)). So the flutter of the upper part of blade can not be obtained.

After the start regime , there began the coupled vibrations where unsteady forces in the turbine stage are the result of continuous interaction between gas flow, rotation of the rotor wheel and blades vibration. So it is impossible to separate the unsteady effects caused by the external excitation and the unsteady effects due to blades vibration.

Figures 3 a, b present the modal components of the unsteady modal force corresponding to the first mode. It is seen that the high frequency excitation appeared for 2800 Hz and is equal to 2% of the steady force A_o=139.1 [N/kg] and for 2* 2800 Hz and is equal to 0.3% of A_o. The low frequency excitation is 0.62% of A_0 for frequency 73 Hz (see Figure 3b).

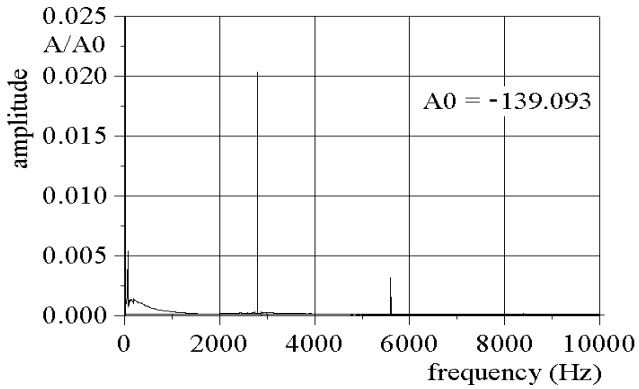

Figure 3a. Amplitude-frequency characteristics for the unsteady modal aerodynamical forces (of the 1st mode) up to 10000 Hz

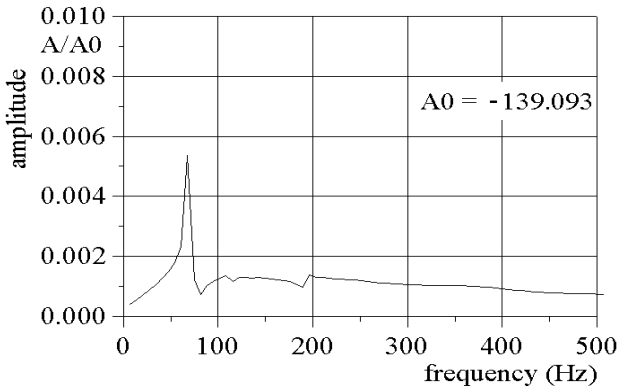

Figure 3b. Amplitude-frequency characteristics for the unsteady modal aerodynamical forces (of the 1st mode) for frequency range up to 500 Hz

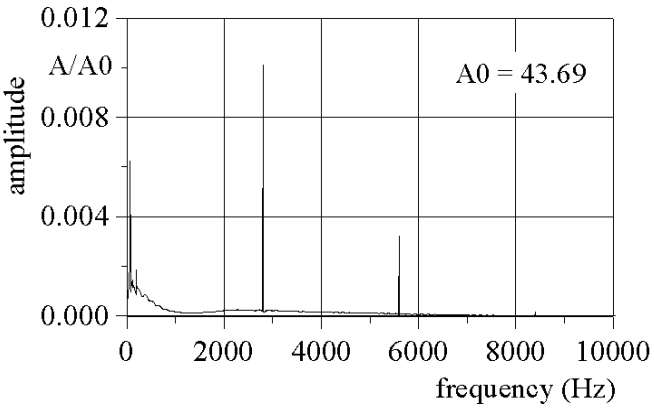

Figure 3c. Amplitude-frequency characteristics for the unsteady modal aerodynamical forces (of the 2nd mode)up to 10000 Hz

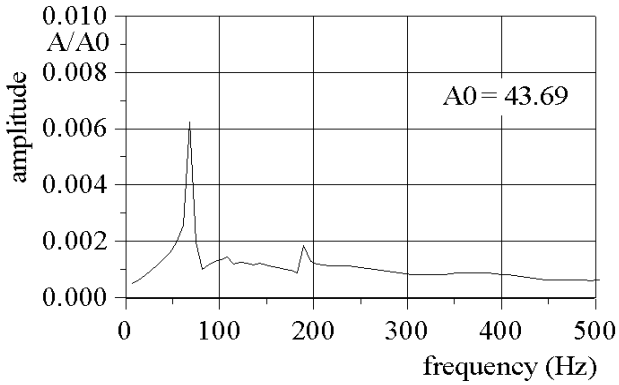

Figure 3d. Amplitude-frequency characteristics for the unsteady modal aerodynamical forces (of the 2nd mode)up to 500 Hz

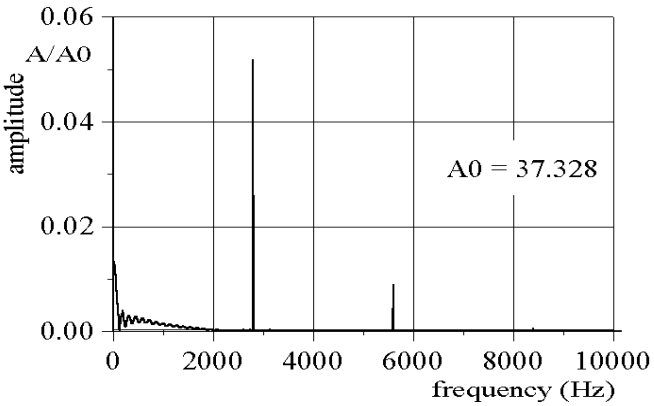

Figure 3e. Amplitude-frequency characteristics for the unsteady modal aerodynamical forces (of the 3rd mode) for frequency range up to 10000 Hz

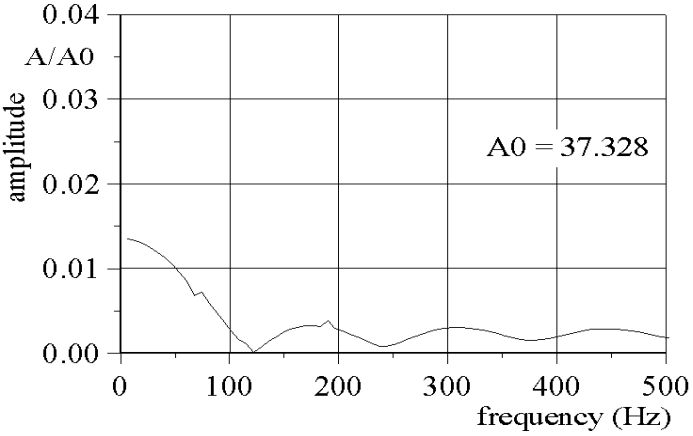

Figure 3f. Amplitude-frequency characteristics of the unsteady modal aerodynamical forces of 3rd mode for frequency range up to 10000 Hz

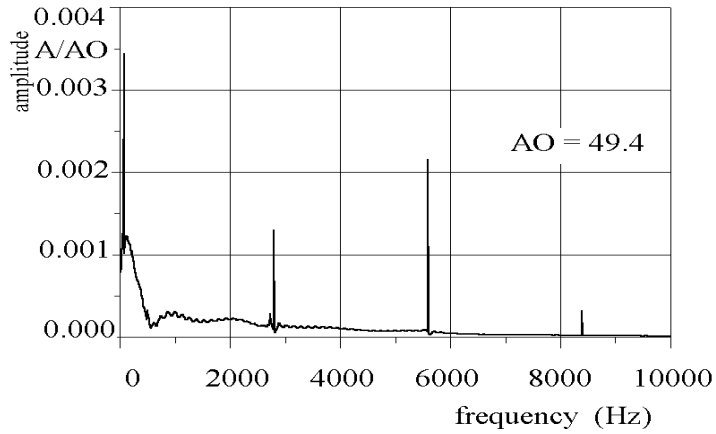

Figure 3g. Amplitude-frequency characteristics for the unsteady modal aerodynamical forces (of the 4th mode) for frequency range up to 10000 Hz

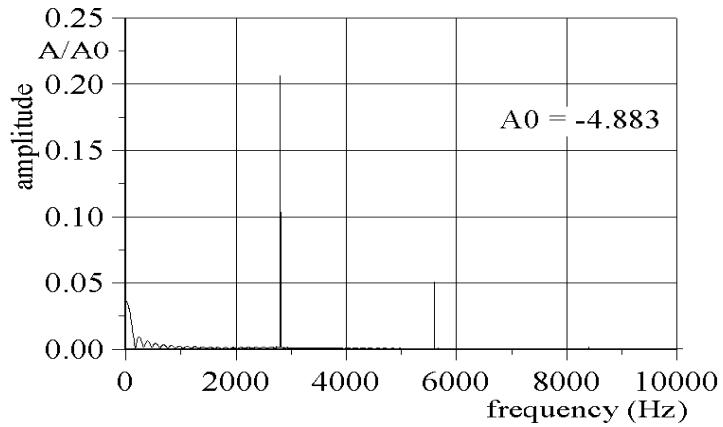

Figure 4a. Amplitude-frequency characteristics for the unsteady modal aerodynamical forces (of the 6th mode) up to 10000 Hz

Figures 3 c, d present the modal components of the unsteady modal force corresponding to the second mode. It is seen that the high frequency excitations appeared for 2800 Hz and is equal to 1% of the steady force A_o=43.67 [N/kg] and for 2* 2800 Hz and is equal to 0.3% of A_o. The low frequency excitation is 0.69% of A_0 for frequency 73 Hz (see Figure 3d) .

Figures 3 e, f present the modal components of the unsteady modal force corresponding to the third mode. It is seen that the high frequency excitations appeared for 2800 Hz and is equal to 5% of the steady force A_o=37.15 [N/kg] and for 2* 2800 Hz and is equal to 1% of A_o=37.15 [N/kg].

Figures 3 g present the modal components of the unsteady modal force corresponding to the fourth mode. It is seen that the high frequency excitations appeared for 2800 Hz and is equal to 0.2% of the steady force A_o=49.4 [N/kg] and for 2* 2800 Hz and is equal to 0.05% of A_o. The low frequency excitation is 0.35% of A_0 for frequency 73 Hz (see Figure 3g). In this case the values of the low frequency excitation is higher then the value of the high frequency excitation.

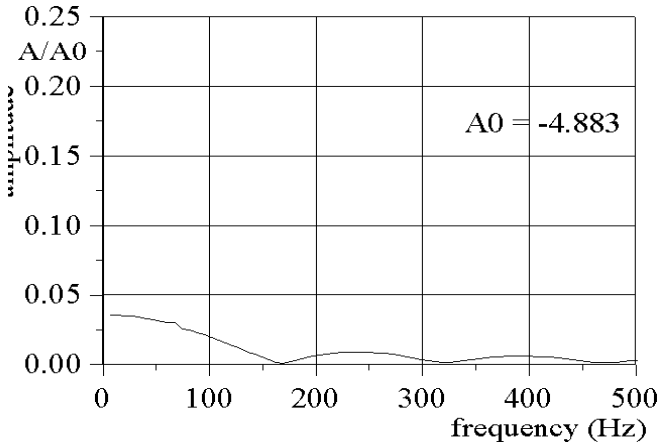

Figure 4b. Amplitude-frequency characteristics for the unsteady modal aerodynamical forces (of the 6th mode) up to 500 Hz

Figures 4 present the modal unsteady components corresponding to the 6th ,8th and 10th modes. The influence of these modes on the valued of the total unsteady modal force is smaller then in the case of the first mode.

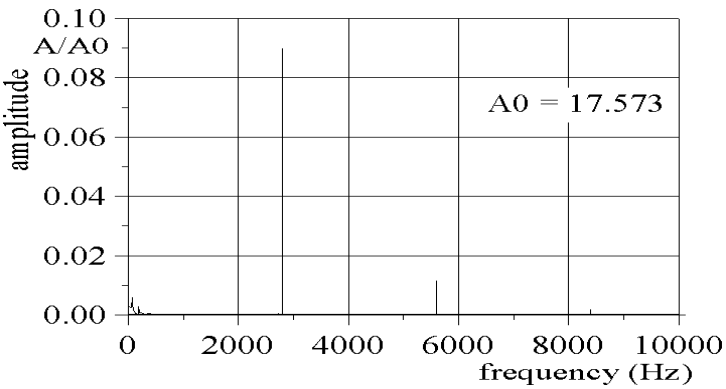

Figure 4c. Amplitude-frequency characteristics for the unsteady modal aerodynamical forces (of the 8th mode)up to 10000 Hz

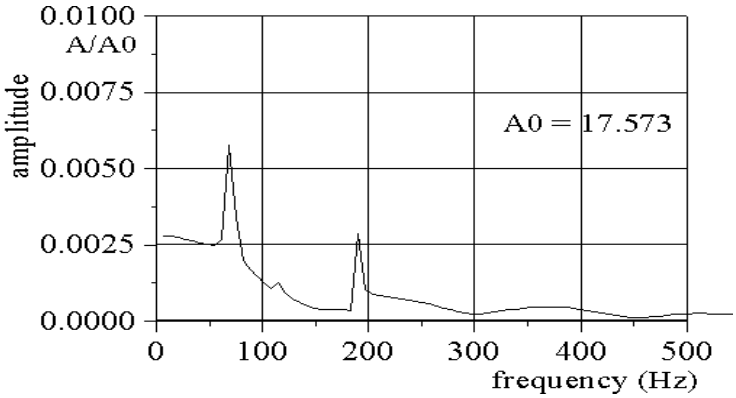

Figure 4d. Amplitude-frequency characteristics for the unsteady modal aerodynamical forces (of the 8th mode) up to 500 Hz

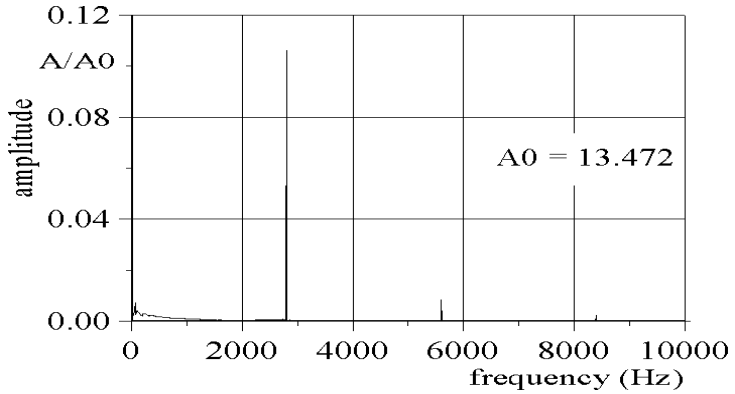

Figure 4e. Amplitude-frequency characteristics for the unsteady modal aerodynamical forces (of the 10th mode) up to 10000 Hz

The values of the unsteady forces calculated for the rotating and non-vibrating blades and rotating and vibrating blades along the blade length are presented in Table 2.

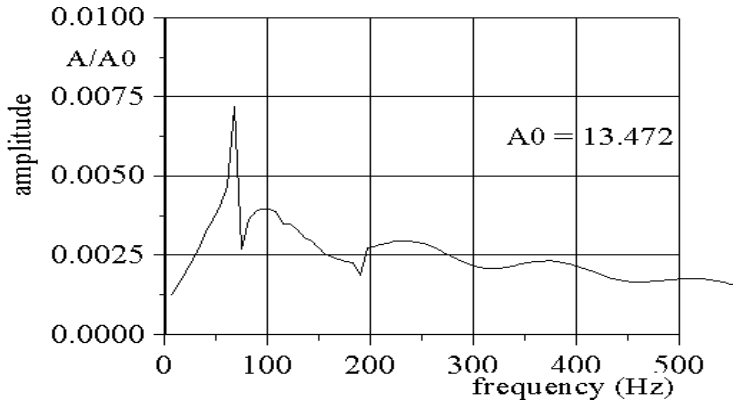

Figure 4f. Amplitude-frequency characteristics for the unsteady modal aerodynamical forces (of the 10th mode) up to 500 Hz

Table 2. The first harmonic components of the unsteady force along the blade length

Non-vibrating	**F_y [%]**	**F_z [%]**	**M [%]**
the peripheral layer	6	4	7
the middle layer	8	3	29
the root layer	39	59	115
Vibrating	**F_y [%]**	**F_z [%]**	**M [%]**
the peripheral layer	7.8	5.4	6
the middle layer	8.2	3	29
the root layer	39	59	115

The blade motion in the form of the modal coefficients variation in time for the 1st and 5th blades is presented in Figures 5a,b,c. The modal coefficients corresponding to the 1st, 2nd, 3rd and 4th modes shape have been shown in Fig. 5a. The integers correspond to mode number. The modal coefficient for 10th mode are presented in Fig. 5b, c.

From this Figures it should be noted:

- only first three modes bring their contribution to the blade motion;
- the logarithmic decrement of oscillations grows with increase of the mode number;
- the interblade phase angle of the blade vibration for the low modes is close to zero and appears for high modes (see Fig. 5 c). The interblade phase angle is different from values 7/6 π (i-1) and is dependant on the natural blade frequency;

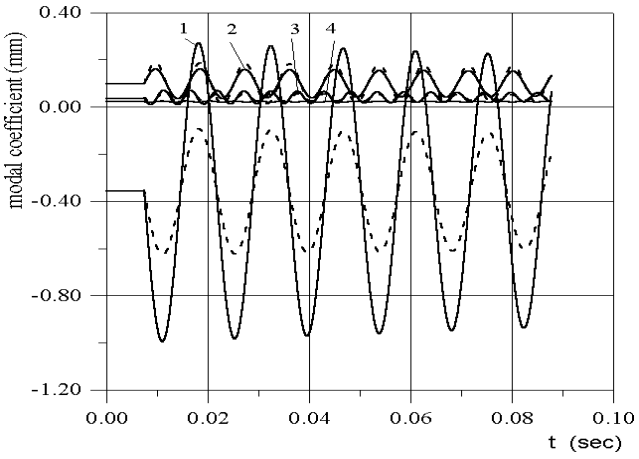

Figure 5a. The modal coefficient during four rotor rotations
_____ 1st blade; ---------- 5th blade

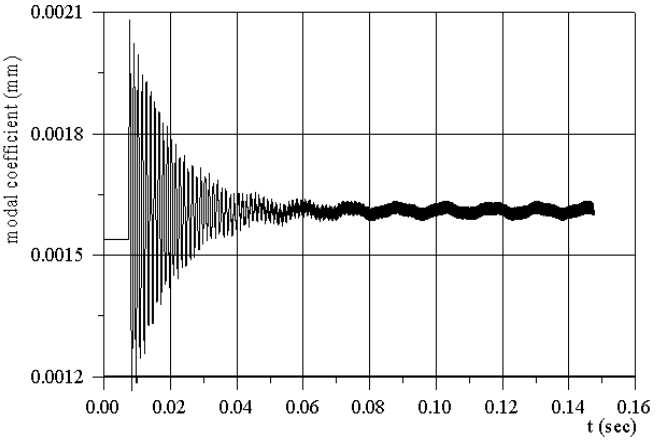

Figure 5b. The 10 th modal coefficient for _____ 1st blade; ---------- 5th blade

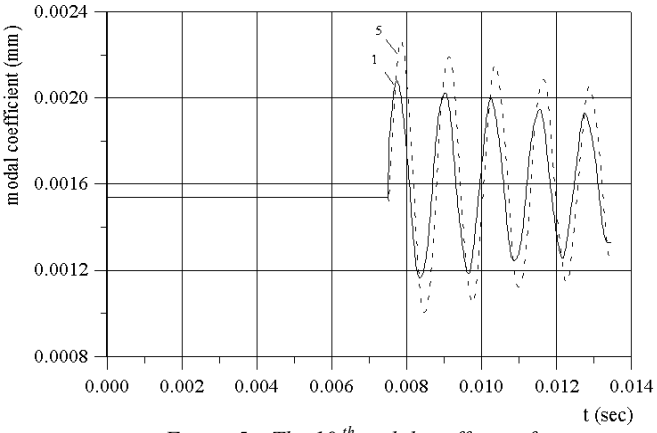

Figure 5c. The 10 thmodal coefficient for _____ 1st blade; ---------- 5th blade

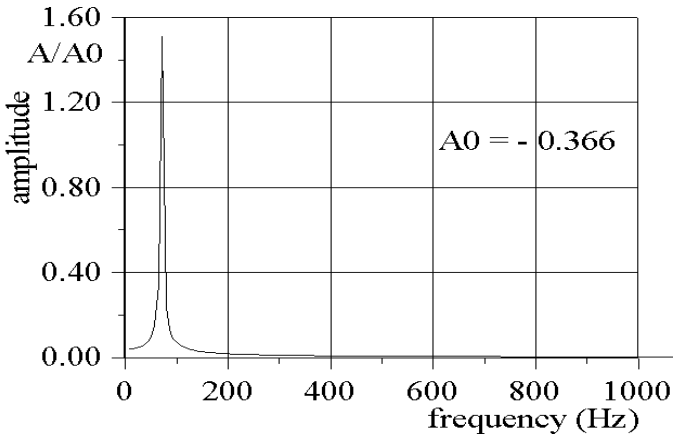

Figure 6a. Amplitude-frequency characteristics for 1st blade motion corresponding to 1st mode shape

The modal coefficients of the 1st blade motion corresponding to the 1st, 2nd, 3rd and 4th modes shape have been shown in Fig. 6a,b,c,d. The modal coefficients corresponding to the 6th, 8th, 10th modes shape have been shown in Fig. 6e, f, g.

The unsteady amplitude of the first mode (see Figure 6a) is 1.4 of the steady amplitude A_o =0.39 mm and has frequency 73 Hz (99Hz the natural frequency). The unsteady amplitude of the second mode (see Figure 6b) is 0.55 of the steady amplitude A_o =0.098 mm and has frequency 117 Hz (160 Hz the natural frequency).

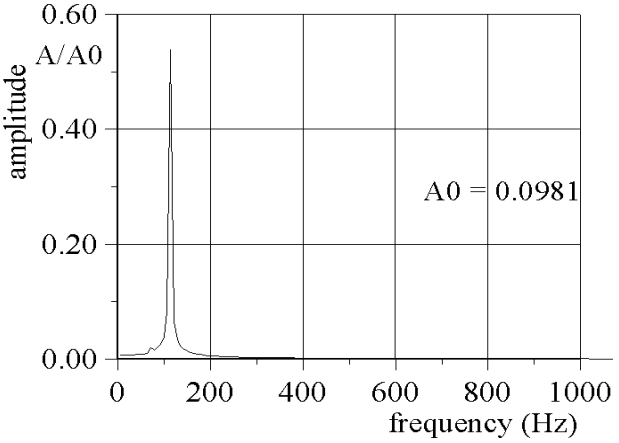

Figure 6b. Amplitude-frequency characteristics for 1st blade motion corresponding to the 2nd mode

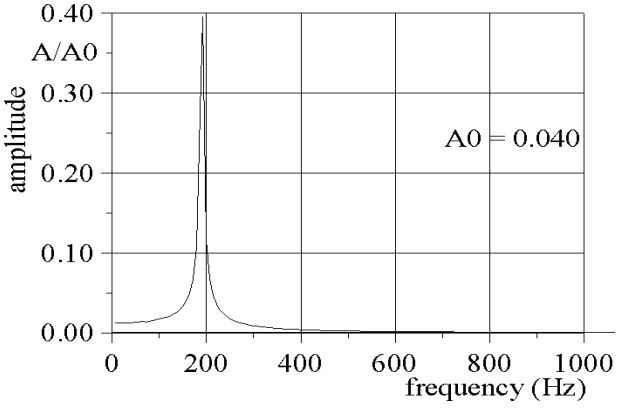

Figure 6c. Amplitude-frequency characteristics for 1st blade motion corresponding to the 3rd mode

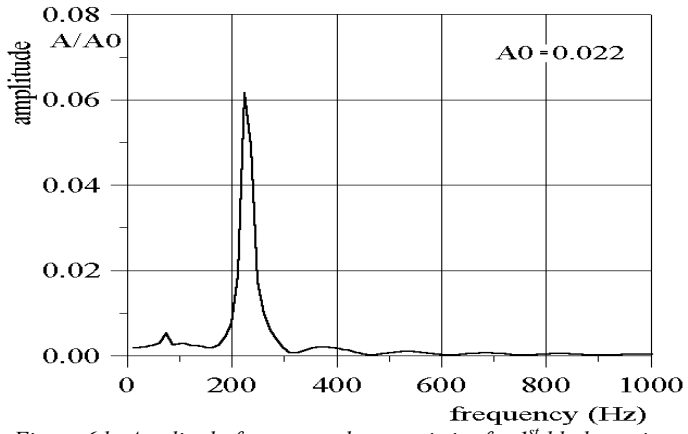

Figure 6d. Amplitude-frequency characteristics for 1st blade motion corresponding to the 4th mode

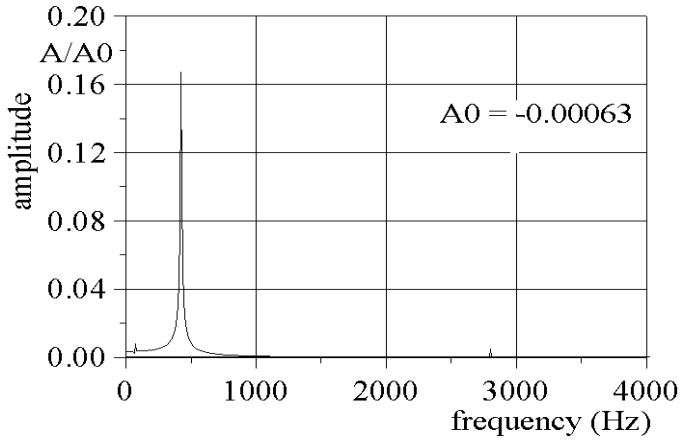

Figure 6e. Amplitude-frequency characteristics for 1st blade motion corresponding to 6th mode

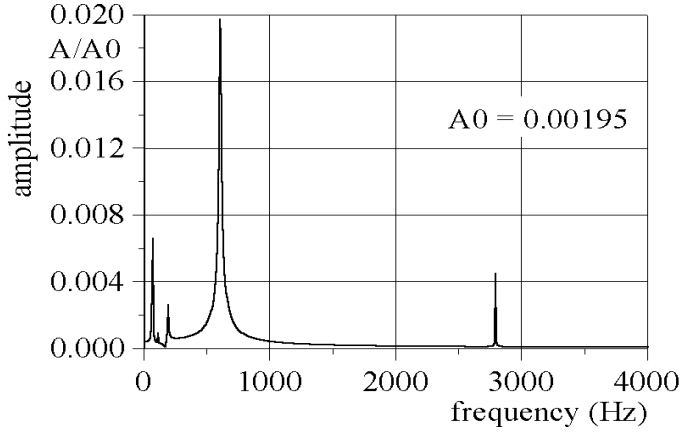

Figure 6f. Amplitude-frequency characteristics for 1st blade motion corresponding to the 8th mode

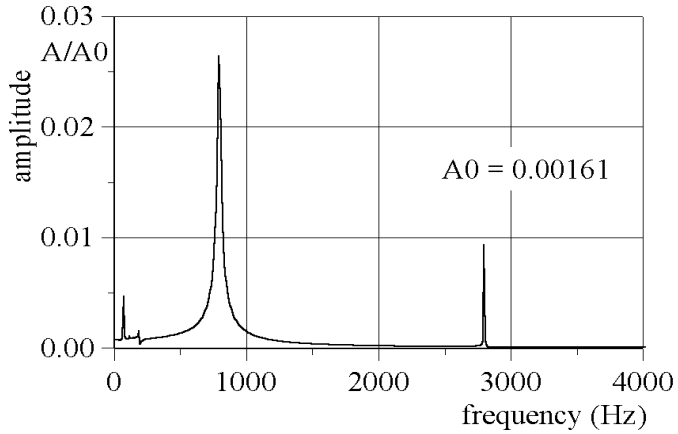

Figure 6g. Amplitude-frequency characteristics for 1st blade motion corresponding to 10th mode

The unsteady amplitude of the third mode (see Figure 6c) is 0.49 of the steady amplitude A_o =0.039 mm and has frequency 188 Hz (268 Hz the natural frequency). The unsteady amplitude of the fourth mode (see Figure 6d) is 0.061of the steady amplitude A_o =0.022 mm and has frequency 214 Hz (297 Hz the natural frequency).

The unsteady amplitude of the sixth mode (see Figure 6e) is 0.17 of the steady amplitude A_o =0.0006 mm and has frequency 375 Hz (598 Hz the natural frequency). The unsteady amplitude of the eight mode (see Figure 6f) is 0.029 of the steady amplitude A_o =0.002 mm and has frequency 600 Hz (863 Hz the natural frequency). The unsteady amplitude of the tenth mode (see Figure 6g) is 0.027 of the steady amplitude A_o =0.00161 mm and has frequency 750 Hz (1124 Hz the natural frequency)

The vibration blade frequencies for different modes in the gas flow is about 30% less then their natural frequencies (see Figs. 6 and Table 1). For example, the blade frequency of the first mode is 73 Hz and the natural frequency is 99 Hz.

CONCLUSIONS

A partially - integrated method based on the solution of the coupled aerodynamic-structure problem is used for calculation of the unsteady 3D flow through a turbine stage with taking into account the rotor blades oscillations.

The paper has investigated the mutual influence of both outer nonuniform flow and blades oscillations. The interblade phase angle of blades oscillations depends not only unsteady forces lag but on the blade natural frequencies, as well (see Figure 5)

It has shown (Figures 6) that amplitude-frequency spectrum includes the harmonics with frequencies which are not multiple to the rotation frequency and close to the natural frequencies of the blades. In case of the first mode (Fig 6a) 73 Hz, natural frequency is 99 Hz , In case of the second mode (Fig 6b) 117 Hz (160 Hz the natural frequency), third mode (Fig 6c) 188 Hz (268 Hz the natural frequency), the fourth mode (Fig 6d) 214 Hz (297 Hz the natural frequency)

Presented results shows the possibility of appearance of the low frequency vibration in the case of mistuning of the rotor, stator blades and any nonuniformity of the inlet or the exit flow

ACKNOWLEDGMENT

The authors wish to acknowledge KBN for the financial support of this work (project 7 T07B 010 16).

All numerical calculations were made at the Academic Computer Centre TASK (Gdańsk, Poland)

REFERENCES

Bakhle, M.A., Reddy, T.S.R., and Keith T.G., 1992, "*Time Domain Flutter Analysis of Cascades Using a Full–Potential Solver"*, AIAA J. vol.30, No 1, p.163.

Bathe K., Wilson E. 1976, "*Numerical Methods in Finite Element Analysis",* Prentice-Hall, Inc Englewood Cliffs , New Jersey.

Bendiksen, O., O., 1998, "*Nonlinear Blade Vibration and Flutter in Transonic Rotors*", Proc. of ISROMAC – 7, The 7th Intern. Symp. on Transport Phenomena and Dynamics of Rotating Machinery, Feb., 22–26, 1998. Honolulu, Hawaii, USA, p. 664.

Carstens V, Belz J., 2000, "*Numerical Investigation of Nonlinear Fluid-Structure Interaction in Vibrating Compressor Blades"*, ASME paper 2000-GT-0381.

Chew J.W., Marshall J.G., Vahdati M. and Imregun M*., 1998 "Part-Speed Flutter Analysis of a Wide-Chord Fan Blade"*, T.H. Fransson(ed.), Unsteady Aerodynamics and Aeroelasticity of Turbomachines, Kluwer Academic Publishers, Printed in the Netherlands. 707-724.

Gnesin, V., I., Rzadkowski R. and Kolodyazhnaya, L., V*.,* 2000, *"A coupled Fluid-Structure Analysis for 3D Flutter in Turbomachines"*, ASME paper 2000-GT-0380.

Gnesin V.I., Rządkowski R., 2000, "*The theoretical model of 3D flutter in subsonic, transonic and supersonic inviscid flow"*, Transaction of the Institute of Fluid-Flow Machinery, No 106, 45-68.

Gnesin V.I. , Rządkowski R., 2001, "*Aeroelastic Behaviour of the Last Stage Steam Turbine Blades. Part II. Coupled Fluid-Structure Oscillations Harmonic Oscillations"*, Transaction of the Institute of Fluid-Flow Machinery, No 107.

Godunov S. K. et al., 1976, "*Numerical Solution of Multidimensional Problems in Gasdynamics",* Nauka, Moscow, 1976 (in Russian).

Hall, K.C. and Silkowski, P.D., 1997, "*The Influence of Neighbouring Blade Rows on the Unsteady Aerodynamic Response of Cascades"*, ASME Journal of Turbomachinery*,* 119,.85-93.

He L., 1984, "*Integration of 2D Fluid / Structure Coupled Systems for Calculation of Turbomachinery Aerodynamic, Aeroelastic Instabilities"*, Journal of Computational Fluid Dynamics. vol.3, p.217.

He L. And Ning W., 1998, "*Nonlinear Harmonic Analysis of Unsteady Transonic Inviscid and Viscous Flows"*, Unsteady Aerodynamics and Aeroelasticity of Turbomachines, proceedings of the 8th International Symposium held in Stockholm, Sweden, Sept. 14-18, 183-189

Marshall, J.G. and Imregun M., 1996, "*A Review of Aeroelasticity Methods with Emphasis on Turbomachinery Applications",* Journal of Fluids and Structures, Vol.10, pp 237-257.

Moyroud F. Jacquet – Richardet G. and Fransson T.H., 1996, "*A Modal Coupling for Fluid and Structure Analysis of turbomachines Flutter. Application to a Fan Stage"*, ASME Paper 96 – GT – 335,.1–19.

Namba, M. and Ishikawa, A., 1983, "*Three-dimensional Aerodynamic Characteristics of Oscillating Supersonic and Transonic Annular Cascades"*, ASME J. of Engineering for Power 105,.138-146.

Rządkowski R., Gnesin V., 2000, *"The Numerical and Experimental Verification of the 3D Inviscid Code",* Transaction of the Institute of Fluid-Flow Machinery, No 106, 2000, 69-95**.**

Rządkowski, R., 1998, "*Dynamics of Steam Turbine Blading, Part Two Bladed Discs",* Ossolineum, Wrocław-Warszawa.

Rządkowski R., Gnesin **V**., 2001, "Aeroelastic Behaviour of the Last Stage Steam Turbine Blades. Part I. Harmonic Oscillations", Transaction of the Institute of Fluid-Flow Machinery, No 107 **.**

Schulten, J.B.H.M., 1982, Sound Generated by Rotor Wakes Interacting with a Leaned Vane Stator, *AIAA J.,*